

# Direct Experimental Evidence for the Hybridization of Organic Molecular Orbitals with Substrate States at Interfaces: PTCDA on Silver

J. Ziroff,<sup>1</sup> F. Forster,<sup>1</sup> A. Schöll,<sup>1</sup> P. Puschnig,<sup>2</sup> and F. Reinert<sup>1,3</sup>

<sup>1</sup>*Universität Würzburg, Experimentelle Physik VII, 97074 Würzburg, Germany*

<sup>2</sup>*Chair of Atomistic Modelling and Design of Materials, University of Leoben, 8700 Leoben, Austria*

<sup>3</sup>*Karlsruher Institut für Technologie, Gemeinschaftslabor für Nanoanalytik, 76021 Karlsruhe, Germany*

(Dated: April 2, 2024)

We demonstrate the application of orbital  $k$ -space tomography for the analysis of the bonding occurring at metal-organic interfaces. Using angle-resolved photoelectron spectroscopy (ARPES), we probe the spatial structure of the highest occupied molecular orbital (HOMO) and the former lowest unoccupied molecular orbital (LUMO) of one monolayer 3,4,9,10-perylene-tetracarboxylic-dianhydride (PTCDA) on Ag(110) and (111) surfaces and in particular the influence of the hybridization between the orbitals and the electronic states of the substrate. We are able to quantify and localize the substrate contribution to the LUMO and thus prove the metal-molecule hybrid character of this complex state.

The adsorption of  $\pi$ -conjugated molecules on metals has attracted considerable interest in surface science due to its importance for the understanding of contacts in organic electronic devices. PTCDA (3,4,9,10-perylene-tetracarboxylic-dianhydride) serves as an archetypical molecule in this field [1–3]. In particular, its behavior in molecular monolayers on Ag surfaces has been studied intensely as a model system for chemisorptive molecule-metal interaction [3–5]. Rich experimental data exist on the geometric structure of these interfaces [5–8], but the bonding distances differ quantitatively from theoretical predictions [9, 10]. Moreover, spectroscopic techniques show a charge transfer from the metal into the lowest unoccupied molecular orbital of the free molecule (LUMO), but the underlying mechanism remains debated. Literature mentions the involvement of several molecular orbitals [4], Ag  $s$ - and  $d$ -bands [11] and additional local bonds forming between the carboxylic O atoms and the Ag surface [8]. Furthermore the Shockley surface state is affected by the PTCDA adsorption and may play a role in the bonding as well [12, 13]. A thorough understanding of the interaction at the interface must be based on the correct description of the valence orbitals. However, information about the spatial distribution of molecular orbitals (MOs) is not easily obtainable. So far scanning tunneling microscopy (STM) is the most direct approach to image surface charge distributions with sub-molecular resolution [3, 9]. Another experimental method is angle-resolved photoelectron spectroscopy (ARPES) [14, 15], since the angular intensity distribution pattern of organic molecules is linked to the wave function geometry of the respective MOs [16, 17]. However, interpretation of ARPES data including final-state scattering [18] based on atomic orbitals is challenging [16]. A new approach has been described very recently [19] which directly links photoemission intensity and initial state wave function, enabling energy resolved tomographic imaging of the electron distribution in  $k$ -space. This allows a direct comparison of experimental and theoretical charge

distribution and a probing of the spatial structure of the bonding orbitals.

In this Letter, we present photoemission data of the two highest occupied interface states of PTCDA on Ag(110) and Ag(111) surfaces and compare our data to free-molecule orbitals as calculated by density functional theory (DFT). We demonstrate the imaging of the respective orbital structure and its correspondence to the free-molecule HOMO/LUMO. Note here that we retain these terms also for the respective orbitals of the adsorbed molecule for simplicity, although the LUMO is not unoccupied anymore (while the HOMO becomes the second occupied MO). Good quantitative agreement is achieved for the spatial distribution of the (non-bonding) HOMO and DFT. The now occupied LUMO deviates from its free-molecule form due to substrate induced modifications. They take the form of an  $s$ -like contribution to the orbital localized laterally at the center of the molecule. Our interpretation of the electronic interaction is compared to quantum-chemical calculations of PTCDA adsorbed on Ag(110) [20] and DFT results for PTCDA on Ag(111) [9]. The experiments were performed in a UHV setup composed of an organic molecular beam epitaxy chamber for sample preparation and a spectrometer chamber for the ARPES measurements (base pressure below  $10^{-10}$  mbar). The Ag substrates have been prepared by standard sputtering and annealing cycles as described elsewhere [21]. PTCDA, purified by triple-sublimation, was evaporated from a Knudsen cell at rates of approximately 0.2 ML per minute onto the substrate which was kept at room temperature. The monolayer coverage was controlled by monitoring the continuous quenching of the Shockley type surface state [22] and the characteristic PTCDA valence band spectra of the chemisorbed monolayer [4]. All ARPES measurements were performed at sample temperatures  $T \approx 80$  K with a high-resolution photoelectron analyzer (Scienta R4000) in combination with a monochromatized VUV lamp using He I $_{\alpha}$  radiation ( $h\nu = 21.23$  eV) at an

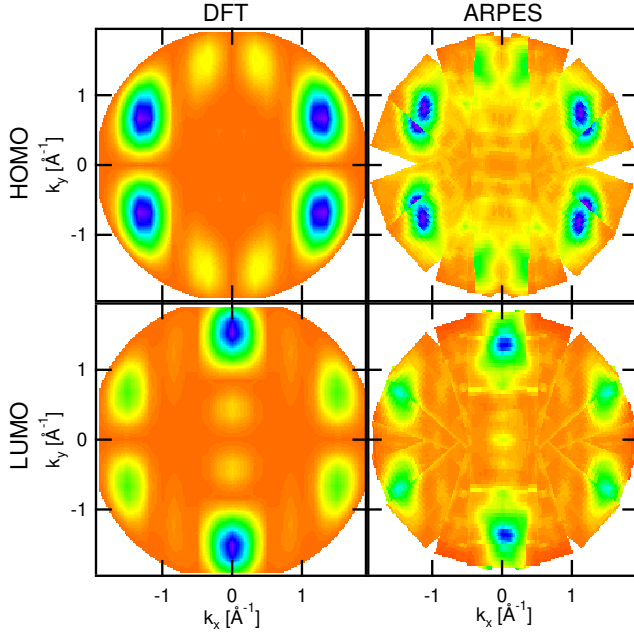


FIG. 1: Right column: Experimental  $k_{x,y}$ -dependent ARPES intensity of the HOMO (top) and LUMO (bottom) of PTCDA on Ag(110) recorded with HeI $\alpha$ . Left column: Corresponding DFT calculations of the free molecule at the respective photoelectron energies.

energy resolution of  $\Delta E = 5$  meV. The angle resolved mode of the analyzer covers a parallel detection range of up to  $\pm 15^\circ$  with a resolution of  $\approx 0.3^\circ$ . An additional rotation of the sample was used to allow 2D  $k$ -space mapping. Molecular orbitals of an isolated PTCDA molecule were calculated within the framework of DFT using the ABINIT software package [23]. Norm-conserving pseudo-potentials with a cut-off of 50 Ryd and a generalized gradient approximation for the exchange-correlation energy and potential have been used. The calculated 2D-ARPES intensity maps are obtained from the Fourier transform of the HOMO and LUMO orbitals at the appropriate kinetic electron energies. Details of this approach are described elsewhere [19].

The monolayer of PTCDA on Ag(110) is a single-domain structure with one molecule per unit cell. The identity of all molecules in terms of adsorption site and absolute orientation allows the effective mapping of MOs without the superposition of additional orientations. The molecule grows on Ag(110) oriented along the [001]-axis of the substrate [24]. We will refer to this direction in momentum space as  $k_x$ , to  $[1\bar{1}0]$  as  $k_y$ . Fig. 1 compares the experimental ARPES intensity (right column) recorded at binding energies of 0.8 eV and 1.9 eV with respect to the Fermi level to the corresponding calculations for the valence MOs (left column). The shown data set was completed from measurements covering one quadrant using the symmetry axis of the system [24]. From the overall

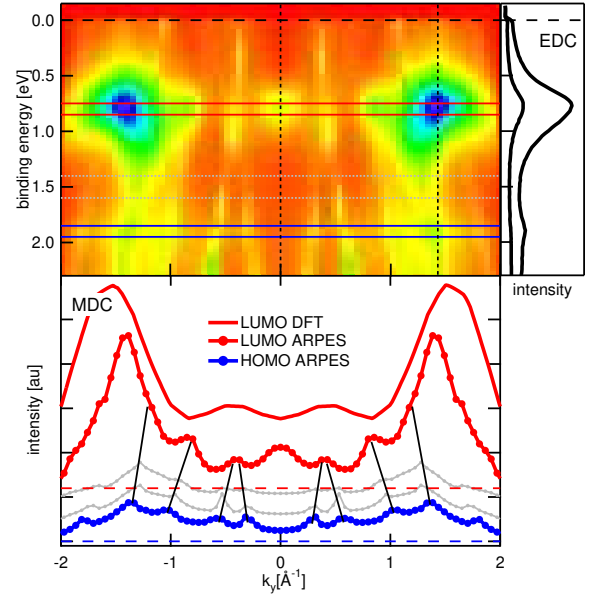


FIG. 2: Top: ARPES intensity vs.  $k_y$  at  $k_x = 0$  for 1 ML PTCDA/Ag(110), EDC for indicated  $k_y$  on the right. Bottom: MDC deduced from the MOs energy windows (red/blue dotted line, dashed line marks respective zero) and at intermediate energies (gray curves). The black lines indicate the dispersing substrate bands. The solid red curve shows the theoretical LUMO intensity (offset from zero for better comparison).

similarity we conclude that the measured orbitals correspond to the HOMO and the LUMO respectively. However, the experimental data exhibits additional photoemission intensity features which do not appear in theory. They are mainly caused by the  $sp$ -bands of the Ag substrate. Fig. 2 (top) shows an energy-resolved ARPES spectrum along the  $k_y$ -direction at  $k_x = 0$  through the momentum map in Fig. 1. The data allows a clear distinction between photoemission intensity from the MOs and the strongly dispersing substrate bands. Selected energy distribution curves (EDC) are displayed on the right. Fig. 2 (bottom) depicts the energy-integrated  $k_y$ -dependent photoemission intensity of the LUMO (red) and the HOMO (blue). Additional line scans (momentum distribution curves (MDC)) at intermediate binding energies (gray lines) are added to visualize the contribution of the Ag bands, black lines guide the eye along the dispersion. The momentum distribution of the HOMO signal is basically featureless, in agreement with theory (cf. Fig. 1). The LUMO signal also generally resembles the free-molecule calculations. However, there is an additional intensity maximum at normal emission ( $k_{||} = 0$ ). Note that this is neither present in the free molecule nor accidentally caused by substrate bands. In addition, the position of the dominating emission maxima at  $k_y \approx 1.6 \text{ \AA}^{-1}$  is shifted to smaller absolute  $k_y$ -values.

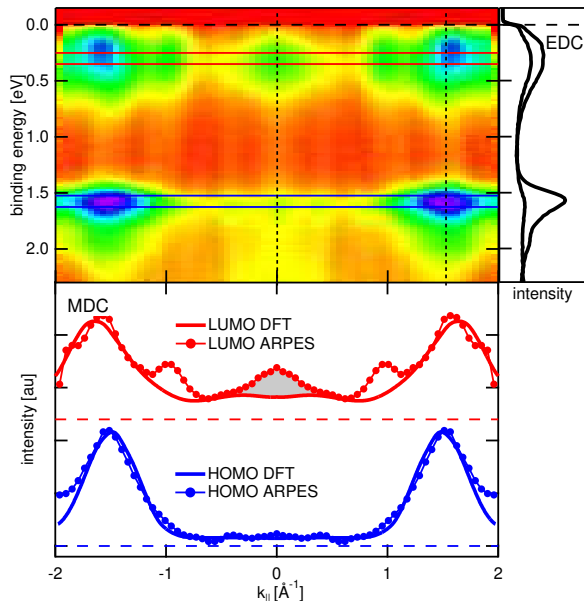


FIG. 3: Top: ARPES intensity vs  $k_{||}$  for 1 ML PTCDA/Ag(111), EDC for indicated  $k_{||}$  on the right. Bottom: MDC of the LUMO (red curve) and HOMO (blue curve) intensity, respective energy windows marked above, zero indicated by dashed line. The solid lines correspond to the calculated DFT intensities (offset from zero). Gray shaded area models the normal emission intensity as Gaussian (FWHM =  $0.42 \text{ \AA}^{-1}$ )

Interpreting our ARPES results for PTCDA on Ag(110), we find the HOMO generally unaltered by the adsorption, therefore we rule out significant substrate admixture to this orbital, the HOMO is apparently not involved in the bonding at the interface. The LUMO generally resembles the free-molecular calculations. However, the shift of the characteristic main intensity maxima to lower  $k_y$  values indicates a distortion of the orbital structure in this direction (i.e. the short molecular axis). Moreover, additional intensity appears around  $k_{||} = 0$ . In real space this would correspond to a laterally node-free charge distribution at the center of the molecule. We therefore suggest a bonding of the molecule due to LUMO hybridization, taking the form of an s-like substrate contribution to the MO at the PTCDA perylene core. A comparison with recent quantum-chemical calculations reconfirms the observed negligible interaction of the HOMO [20]. For the LUMO, a distortion along the short molecular axis and additional substrate-localized lobes are visible in the calculated orbital structure [20], matching our experimental findings. However, the calculations show a node (and therefore a parity change) of the hybrid orbital along the  $k_x$  axis, a prediction which is not compatible with the experimentally observed normal emission intensity.

In contrast to the (110) surface, PTCDA on Ag(111) forms a multi-domain herringbone structure. Six sym-

metry equivalent domains with two molecules per unit cell [3] result in twelve different molecule orientations. Therefore, measuring the polar-angle dependence of the PE intensity effectively means probing the averaged  $k_{||}$ -dependence of the MOs. While this reduces the 2D-maps into one-dimensional data sets it gives two advantages: On the one hand a more complex geometry of the organic overlayer prevents an overlap with intense *sp*-bands due to backfolding [22]. On the other hand one measures all data points at an identical geometry between photon source and the emitted electrons, allowing for a strict quantitative analysis of the MDC in terms of electron distribution of the initial MO, since the modulating polarization factor  $\mathbf{A} \cdot \mathbf{k}$  remains constant [19]. Fig. 3 presents energy and  $k_{||}$  resolved photoemission intensity for a monolayer of PTCDA/Ag(111) (top, data symmetrized to  $k_{||} = 0$ ). The MDCs of the background corrected LUMO and HOMO (red and blue energy window) are compared to the free-molecule DFT results in the bottom panel. The theoretical data was averaged over the azimuthal angle (emulating the multiple domains in the experiment) and offset from zero to allow for a constant experimental intensity. The HOMO is again characterized by a single, dominating maximum. The deviation for higher  $k$ -values is probably caused by the grazing incidence of the light and high electron emission angle ( $\Theta \approx 70^\circ$ ), setting an upper  $k$  limit for quantitatively reliable measurements in our experimental setup. Otherwise, the agreement between free-molecule theory and experiment is excellent. From this we conclude an undistorted HOMO geometry and a weakly interacting character of this MO on Ag(111), analogous to the Ag(110) substrate. For the LUMO, a slight inward shift of the dominating maxima is observed, as is again ARPES intensity at  $k_{||} = 0$ . From this we deduce a similar bonding mechanism as described for Ag(110) above. There is, however, also a distinctive new peak at  $k_{||} \approx \pm 0.9 \text{ \AA}^{-1}$ , neither present in the DFT calculations nor a feature of the substrate. It corresponds to a real-space periodicity of  $7 \text{ \AA}$  in the LUMO structure. This value is almost twice as large as the typical node-distance within the undistorted MO (causing the dominating ARPES intensity maxima) and comparable to the lateral PTCDA dimensions ( $9.2 \times 14.2 \text{ \AA}$ ) [3]. This length scale hints at a charge redistribution over the single PTCDA molecule, possibly due to inter-molecular interaction. On Ag(111) PTCDA arranges in a herringbone structure with a nearest-neighbor distance below the van der Waals radii of the molecules, caused by electrostatic forces acting between the negatively charged anhydride group and the aromatic core region [3]. Such an interaction could cause the observed modifications in a strongly delocalized bonding orbital like the LUMO. Another indication is the absence of the considered ARPES feature in the previously discussed data for the Ag(110) surface, on which the PTCDA molecules are distinctly separated

from each other on specific adsorption sites. In order to quantitatively analyze the additional normal-emission intensity, we approximate it by a Gaussian as displayed by the shaded area in Fig. 3. The real-space correspondence is a node-free charge spread laterally (FWHM  $\approx 7$  Å) over the central part of the PTCDA perylene core. A first estimate assigns  $\approx 10$  % of the total PE intensity to the area around  $k_{\parallel} = 0$ , a value which may provide a measure for the substrate contribution to the PTCDA-Ag hybrid state. Quantum-chemical calculations for PTCDA/Ag(110) state a comparable (16 %) substrate contribution [20]. A detailed comparison with theoretical calculations for PTCDA on Ag(111) is not directly possible, there are only projected charge densities for PTCDA/Ag(111) obtained by DFT calculations [9]. They describe the lateral distribution between the molecule and the substrate as an undistorted LUMO with additional charge accumulated around the central carbon ring of the molecule [2]. This description resembles the electron probability density that would result from the orbital geometries deduced from our data.

In conclusion, we demonstrate the potential of orbital tomography by ARPES for the comprehensive understanding of the fundamentals of the bonding of large organic molecules to surfaces. On the particular example of the PTCDA molecule, chemisorbed on Ag surfaces, we show that the HOMO orbital does not show a significant substrate admixture. It is therefore not decisively involved in the molecule-substrate bonding. In contrast, the LUMO features a significant distortion of the orbital spatial structure compared to the free-molecule and a prominent admixture of substrate states. A first analysis estimates the substrate contribution to the LUMO as  $\approx 10\%$ , localized in a node-free charge accumulation at the central carbon ring of the perylene core. Our results are in good agreement with quantum-chemical calculations for the MOs of PTCDA on Ag(110) and DFT calculations for PTCDA on Ag(111), with the exception of the nodal structure of the LUMO hybridization on Ag(110).

This work was supported by the Bundesministerium für Bildung und Forschung (BMBF) under grants 05KS7FK2/05KS7WW1 and 035F0356B and by the Deutsche Forschungsgemeinschaft (DFG) via FOR1162. P.P. acknowledges support from the Austrian Science Foundation (FWF) within the national research network S97.

- [2] F. S. Tautz, *Progress in Surface Science* **82**, 479 (2007).
- [3] K. Glöckler, C. Seidel, A. Soukopp, M. Sokolowski, E. Umbach, M. Böhrringer, R. Berndt, and W. D. Schneider, *Surface Science* **405**, 1 (1998).
- [4] Y. Zou, L. Kilian, A. Schöll, T. Schmidt, R. Fink, and E. Umbach, *Surface Science* **600**, 1240 (2006).
- [5] M. Böhrringer, W. D. Schneider, K. Glöckler, E. Umbach, and R. Berndt, *Surface Science* **419**, L95 (1998).
- [6] D. Braun, A. Schirmeisen, and H. Fuchs, *Surface Science* **575**, 3 (2005).
- [7] L. Kilian, A. Hauschild, R. Temirov, S. Soubatch, A. Schöll, A. Bendounan, F. Reinert, T. L. Lee, F. S. Tautz, M. Sokolowski, et al., *Physical Review Letters* **100**, 136103 (2008).
- [8] A. Hauschild, K. Karki, B. C. C. Cowie, M. Rohlfling, F. S. Tautz, and M. Sokolowski, *Physical Review Letters* **94**, 036106 (2005).
- [9] M. Rohlfling, R. Temirov, and F. S. Tautz, *Physical Review B* **76**, 115421 (2007).
- [10] L. Romaner, D. Nabok, P. Puschnig, E. Zojer, and C. Ambrosch-Draxl, *New Journal of Physics* **11**, 053010 (2009).
- [11] E. Kawabe, H. Yamane, R. Sumii, K. Koizumi, Y. Ouchi, K. Seki, and K. Kanai, *Organic Electronics* **9**, 783 (2008).
- [12] C. H. Schwalb, S. Sachs, M. Marks, A. Schöll, F. Reinert, E. Umbach, and U. Höfer, *Physical Review Letters* **101**, 146801 (2008).
- [13] R. Temirov, S. Soubatch, A. Luican, and F. S. Tautz, *Nature* **444**, 350 (2006).
- [14] F. Reinert and S. Hufner, *New Journal of Physics* **7**, 97 (2005).
- [15] Y. Azuma, S. Akatsuka, K. K. Okudaira, Y. Harada, and N. Ueno, *Journal of Applied Physics* **87**, 766 (2000).
- [16] S. Kera, S. Tanaka, H. Yamane, D. Yoshimura, K. K. Okudaira, K. Seki, and N. Ueno, *Chemical Physics* **325**, 113 (2006).
- [17] S. Kera, H. Yamane, H. Fukagawa, T. Hanatani, K. K. Okudaira, K. Seki, and N. Ueno, *Journal of Electron Spectroscopy and Related Phenomena* **156**, 135 (2007).
- [18] J. Osterwalder, T. Greber, P. Aebi, R. Fasel, and L. Schlapbach, *Physical Review B* **53**, 10209 (1996).
- [19] P. Puschnig, S. Berkebile, A. J. Fleming, G. Koller, K. Emtsev, T. Seyller, J. D. Riley, C. Ambrosch-Draxl, F. P. Netzer, and M. G. Ramsey, *Science* **326**, 702 (2009).
- [20] A. Abbasi and R. Scholz, *Journal of Physical Chemistry C* **113**, 19897 (2009).
- [21] G. Nicolay, F. Reinert, S. Schmidt, D. Ehm, P. Steiner, and S. Hufner, *Physical Review B* **62**, 1631 (2000).
- [22] J. Zirosso, P. Gold, A. Bendounan, F. Forster, and F. Reinert, *Surface Science* **603**, 354 (2009).
- [23] X. Gonze, J. M. Beuken, R. Caracas, F. Detraux, M. Fuchs, G. M. Rignanese, L. Sindic, M. Verstraete, G. Zerah, F. Jollet, et al., *Computational Materials Science* **25**, 478 (2002).
- [24] C. Seidel, C. Awater, X. D. Liu, R. Ellerbrake, and H. Fuchs, *Surface Science* **371**, 123 (1997).